

Influence of large-scale teleconnection patterns on methane sulfonate ice core records in Dronning Maud Land

Felix Fundel,¹ H. Fischer,¹ R. Weller,¹ F. Traufetter,^{1,2} H. Oerter,¹ and H. Miller¹

Received 14 February 2005; revised 31 October 2005; accepted 17 November 2005; published 25 February 2006.

[1] Records of methane sulfonate (MS^-) in ice cores from the high plateau of Dronning Maud Land (DML), Antarctica, drilled in the framework of the European Project for Ice Coring in Antarctica, are investigated for their potential as an environmental and climate archive for the Atlantic sector of the Southern Ocean. Despite postdepositional changes, years of extraordinary MS^- concentrations can be clearly detected in the ice core records. We use composite anomaly maps of atmospheric parameters from the National Centers for Environmental Prediction/National Center for Atmospheric Research reanalysis fields for years of extreme MS^- concentration to detect atmospheric patterns causing MS^- variability. Changing atmospheric transport is shown to be an important, but not exclusive, parameter being conserved in the MS^- record in DML. The often hypothesized direct link between high MS^- concentrations and El Niño events is not supported for the observed region whereas the Antarctic Dipole (ADP), which is modulated by El Niño–Southern Oscillation conditions, exerts significant influence. A clear 13.9-year cycle can be found throughout a 2000-year MS^- record that can be related to variations in the ADP. Over the last 300 years a 4.6-year cycle is revealed in the MS^- (and sea-salt record), which vanishes in the deeper part of the ice core as a consequence of diffusion processes. From the long-term perspective, periods of high MS^- concentrations are connected to, on average, higher sea-salt aerosol as well, reflecting a seasonally independent influence of transport on both species. A distinctive period of efficient atmospheric transport, probably due to a pronounced ADP, could be found from 1200 to 1600 A.D.

Citation: Fundel, F., H. Fischer, R. Weller, F. Traufetter, H. Oerter, and H. Miller (2006), Influence of large-scale teleconnection patterns on methane sulfonate ice core records in Dronning Maud Land, *J. Geophys. Res.*, *111*, D04103, doi:10.1029/2005JD005872.

1. Introduction

[2] The marine biosphere plays an important role in the climate system as the fate of atmospheric carbon dioxide is strongly coupled to the marine primary production [Kohfeld *et al.*, 2005, and references therein] and marine biogenic aerosol is directly and indirectly (via cloud formation) influencing the radiation budget of the Earth [Andreae and Crutzen, 1997; Ayers and Gillett, 2000]. Accordingly, ice core records of marine biogenic aerosol tracers such as SO_4^{2-} and especially methane sulfonate (MS^-), which is solely of marine biogenic origin, have attracted increasing attention as potential records of marine productivity and radiative forcing in the past [Gondwe *et al.*, 2003].

[3] The ultimate source of these aerosol species is dimethylsulfoniopropionate (DMSP), which is used by phytoplankton as organic osmosis regulator [Brown, 1976], but also as grazing deterrent [Wolfe *et al.*, 1997] because of its antibacterial effects [Sieburth, 1960], as cryoprotection

[Karsten *et al.*, 1996] and against oxidative stressors [Sunda *et al.*, 2002]. With cell death the DMSP becomes released to the ocean where it is cleaved to dimethylsulfide (DMS). As DMS is highly volatile it is released to the atmosphere, where it undergoes complex and not yet fully quantified oxidation pathways to MS^- and SO_4^{2-} [von Glasow and Crutzen, 2004]. Similar to its precursor DMSP the main production time for MS^- in the Southern Hemisphere is the austral summer [Gondwe *et al.*, 2003], when the algae bloom approaches its end. The atmospheric oxidation pathway of DMS can be generally divided in an addition and an abstraction branch. MS^- can be produced via both pathways by oxidation with OH, BrO or NO_3 radicals when available. The aerosol ratio of MS^- to sulfate produced by the marine biosphere is found to be about 0.3 [Bates *et al.*, 1992], but this number is highly variable and because of its dependence on the availability of radicals also strongly related to ambient conditions of the respective observation site.

[4] There have been several attempts in using MS^- as a proxy for atmospheric or environmental change. For example, Curran *et al.* [2003] have shown a clear relation of MS^- and sea ice extent (SIE), for the past ~25 years at the coastal high-accumulation site Law Dome, where the time and extent of sea ice retreat has an impact on the

¹Alfred Wegener Institute for Polar and Marine Research, Bremerhaven, Germany.

²Now at Prinsengracht, Amsterdam, Netherlands.

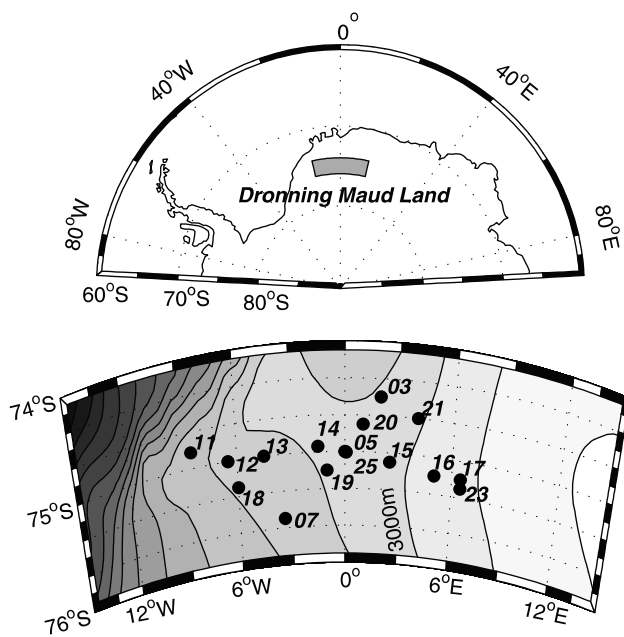


Figure 1. Area of investigation in Dronning Maud Land, Antarctica. Enlargement shows the locations and names of the snow pits and cores used [Oerter *et al.*, 1999, 2000]; the contour lines show the site elevation in meters above sea level in 200-m intervals.

development of algae blooms. At other coastal Antarctic sites such as Neumayer MS^- shows a well pronounced seasonal cycle with maximum in austral summer that fits the nss-SO_4^{2-} very well [Minikin *et al.*, 1998]. Also connections of El Niño events with extraordinarily high MS^- concentrations were suggested in former ice core aerosol studies [e.g., Isaksson *et al.*, 2001; Legrand and Feniet-Saigne, 1991; Meyerson *et al.*, 2002].

[5] The use of MS^- in ice cores as proxy for past production of DMS by algae, however, is hampered, by postdepositional changes in the snow pack. For low-accumulation sites, postdepositional processes like diffusion, migration and loss of volatile species such as MS^- via the gas phase become increasingly more important [Curran *et al.*, 2002; de Angelis and Legrand, 1995; Delmas *et al.*, 2003; Legrand *et al.*, 1996; Röthlisberger *et al.*, 2002, 2003; Wagnon *et al.*, 1999]. In fact, it may be questioned whether there is any atmospheric net signal left in the MS^- records or at least whether the signal/noise ratio is high enough to achieve reliable results. For example the ice core drilled during 1998 and 1999 at Dome C, Antarctica, shows effects like peak broadening of weak acids [Barnes *et al.*, 2003]. This in principle holds for MS^- as well and has been clearly observed for seasonally high acid layers in ice cores from the Filchner-Ronne ice shelf [Minikin *et al.*, 1994]. In addition, ice core studies at Vostok showed decreasing MS^- concentrations in the top layers and very low concentrations in the upper 50 m that have been attributed to a net loss of MS^- from the firn column as well as loss due to improper storage [Delmas *et al.*, 2003].

[6] On the basis of snow pit studies in DML, Weller *et al.* [2004] only recently showed unequivocally that on average, $51 \pm 20\%$ of the MS^- once contained in the surface snow is

lost within the first 1 to 2 m. Thus net loss and diffusional smoothing of MS^- in ice cores makes the interpretation of MS^- time series in terms of atmospheric transport or past variation in DMS production a difficult task. However, as long as initially high concentrations of MS^- in the top firn layers remain peaks when propagating to deeper layers with time, a reconstruction at least of parts of the atmospheric variability should be possible. Accordingly, in this study we attempt to quantify the remnant net information contained in the MS^- records from DML firn cores. Furthermore, we try to assign variability in MS^- to certain teleconnection patterns.

2. Ice Core Data

[7] In order to quantify the spatial representativeness of the variability in MS^- concentrations, snow pits and shallow ice cores from the high-plateau area of DML, Antarctica (Figure 1; precise coordinates and altitudes are given by the Pangaea database (<http://www.pangaea.de>) and partly by Göktaş *et al.* [2002]), have been drilled and excavated at altitudes up to 3000 m above sea level (a.s.l.) within the framework of the EPICA pre-site survey during the austral summer seasons 1997/1998 to 2002/2003. Here, the long-term temporal variability in MS^- concentrations in the late Holocene is quantified using a medium depth core drilled at DML05 (75°00'S, 0°00'E, 2882 m a.s.l., further on referred to as DML05 core), reaching a depth of 148.8m as described by Göktaş *et al.* [2002]. Further on, recent MS^- concentration records are taken from the medium depth cores from DML03, -07 and -17 as well as from the snow pits shown in Figure 1. Within the sample sites the mean accumulation rate varies from 4.7 (DML17) up to 8.9 (DML03) cm water equivalent yr^{-1} [Göktaş *et al.*, 2002]. Air back trajectory studies by Reijmer *et al.* [2002] show that on average, air parcels and precipitation events at DML originate in the Southern Atlantic Ocean between 50°S and 60°S four days prior to their arrival on the DML plateau. This is supported by model studies from Cosme *et al.* [2005] and makes DML a unique region for investigations of past changes in biogeochemistry of the Atlantic sector of the Southern Ocean (SO). Most of the precipitation (about 80%) is caused by frontal clouds [Reijmer *et al.*, 2002]. Model studies of the past 15 years show a roughly uniform distribution of precipitation throughout the year with a slight maximum in late summer to early winter [Reijmer *et al.*, 2002].

[8] The intermediate depth cores drilled at DML03, -05, -07 and -17 were stratigraphically dated using high-resolution chemistry records together with volcanic eruption markers in the sulphate record [Sommer *et al.*, 2000; Traufetter *et al.*, 2004]. For the DML05 core the dating uncertainty is better than ± 5 years for the upper 1000 years and increases steadily to up to 25 years at the bottom of the core (approximately 165 A.D.) because of the lack in reliable dates of historic volcano eruptions [Traufetter *et al.*, 2004]. The snow pits were also dated stratigraphically using high-resolution $\delta^{18}\text{O}$ profiles and snow chemistry records. In this study we use the MS^- concentration time series of the intermediate cores in annual resolution. The equidistant yearly resolution was achieved by calculation of annual mean concentrations. Because of the uniform distri-

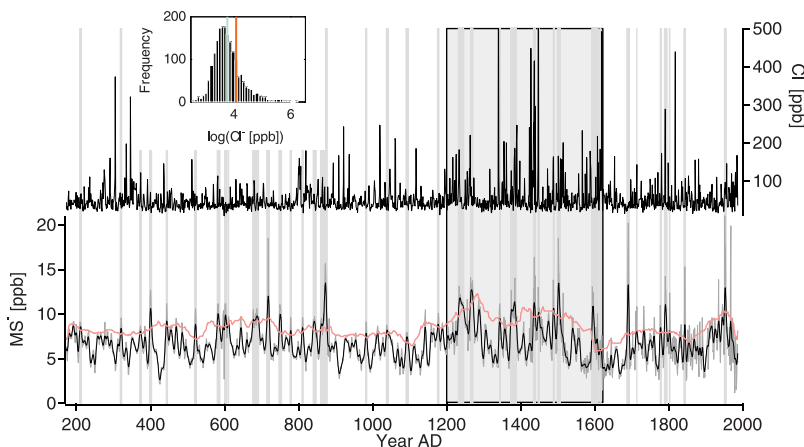


Figure 2. MS^- and Cl^- (plot cut off at 500 ppb) from the medium-depth core at DML05. The MS^- record (grey line) is overlain by a 5-year Gaussian-weighted filter (black line) to avoid an exceeding influence of the more variable younger part on the peak detection. The pink line shows the peak detection threshold as described in the text. The grey lines mark periods of outstanding high MS^- concentrations; the shaded box envelopes a period of enhanced MS^- concentration and frequent Cl^- peaks. The inlay shows frequency distribution of $\log(\text{Cl}^-)$: The overall mean and the mean of extreme MS^- years are marked by the green and red lines, respectively.

bution of precipitation a bias toward any season is not expected.

[9] MS^- and Cl^- concentrations were determined using suppressed ion chromatography as described in detail by *Göktas et al.* [2002] and *Traufetter et al.* [2004]. Anions were measured using a Dionex AS11 column and 0.5–16 mM KOH eluent. Absolute quantification was assured by measuring 7 standard solutions approximately every 50 samples. The total reproducibility (including blank variability) is better than approximately 5% for all anions, with reproducibility becoming better for higher concentrations, where blank variability becomes insignificant. For MS^- the blank contribution is below the detection limit.

[10] A basic assumption of most methods in time series analysis is the normal distribution of the record. As contamination effects for MS^- are unlikely, no outliers were removed but logarithmic concentrations were used for time series analysis to ensure normal distribution of the data. Figure 2 shows the MS^- and Cl^- records of the medium-depth core at DML05.

3. Results and Discussion

3.1. Spectral Analysis

[11] As clearly shown [*Curran et al.*, 2002; *Delmas et al.*, 2003; *Legrand et al.*, 1996; *Wagnon et al.*, 1999; *Weller et al.*, 2004] MS^- records are subject to diffusional smoothing and postdepositional net loss in the firn column, the latter being strongly dependent on snow accumulation rate. Because the snow accumulation in the past has been reconstructed in our ice cores a correction for loss process is in principle possible (e.g., according to *Weller et al.* [2004]). Also diffusional smoothing could be removed by back diffusion methods. However, correction for both processes will introduce large errors on interannual to decadal timescales, for example, due to the strong noise in annual accumulation data, and seems not advised if interpretation on these timescales is intended. Furthermore, the record of

snow accumulation in the DML05 core shows no long-term trend, excluding any long-term bias in the MS^- record. Accordingly, we start by analyzing the remnant spectral properties of the MS^- record after loss and diffusion, as directly measured on the ice cores.

[12] Power spectra of the logarithmic MS^- data were calculated using the Maximum Entropy Method (MEM) because of its advantages in spectral resolution and detecting harmonics near the length of the record [*Ghil et al.*, 2002]. A Monte Carlo routine, based on a first-order autoregressive process fitted to the data, was used to test the peaks in the spectra for their significance. The MEM is applied in two complementary ways. On the one hand the global spectrum using the entire time series is calculated to provide information about quasi-periodic variability dominating the whole record. Alternatively, the MEM is used in an evolutionary way. To this end, the time series is divided in overlapping windows of equal size and the spectrum is calculated separately for each window. Thus temporal tracking of dominant periodicities is possible at the expense of the resolution of long cycles. To make a comparison of the power spectra of each window possible despite of decreasing variance by loss and diffusion processes, the data are normalized to unit variance and the linear trend was removed before calculating the spectra. For scaling convenience the spectra are normalized to the spectra of the underlying first-order autoregressive process AR(1), which emphasizes the high-frequency part in Figure 3a but does not change the significance of appearing cycles.

[13] The global spectrum of MS^- from DML05 (Figure 3a, right) shows periodicities (significant on the 99% level) between 3 and 20 years. Regarding the evolutionary spectrum (Figure 3a, left), a continuous significant oscillation emerges with maximum power at 13.9 years. In addition, the younger part of the evolutionary spectrum contains shorter periods that are soon diminished, because of MS^- diffusion in the open pore space of the firn column.

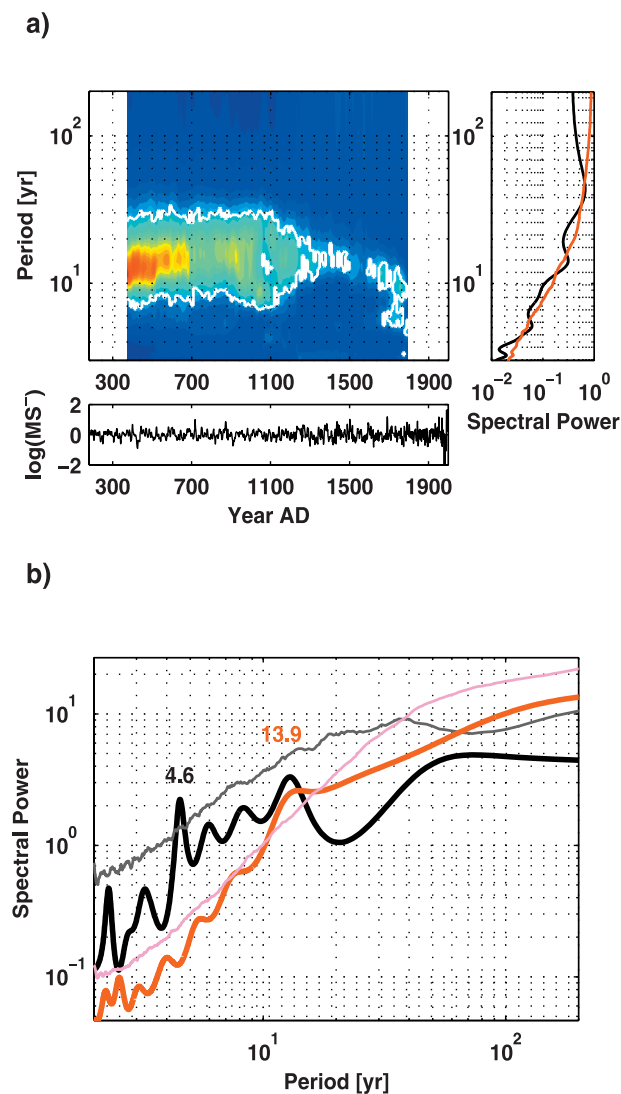


Figure 3. (a) Evolutionary MEM spectrum of $\log(\text{MS}^-)$. Window size is 400 years, and MEM is of order 10; solid white lines represent the 99% significance level. The right plot shows the global MEM spectrum and the 99% significance level. Both spectra are normalized by the spectrum of the underlying AR(1) process. The lower plot shows the logarithmic MS^- time series from DML05. Low-frequency variability above the window length was removed from the MS^- time series by applying a Gaussian filter function. (b) Power spectrum (MEM order 20) on the recent 300 years (black) and the oldest 1500 years (red) of $\log(\text{MS}^-)$ from DML05. The thin grey and pink lines show the 99% confidence levels for each time series, found by the MC test as described in the text. Using other methods for spectral analysis (e.g., Thomson multitaper method [Thomson, 1982]) gives essentially the same results.

Further loss of variability is suppressed below 70–80 m (1400 A.D.) after the bubble close off in firm.

[14] To illustrate the spectral behavior of the youngest 400 years of MS^- concentrations in the DML05 core, where higher frequencies are still detectable, MEM spectral analysis was applied to this period separately (Figure 3b). A

highly significant ($p < 0.01$) cycle at 4.6 years is dominating this part of the time series. Consistent with the evolutionary spectrum a peak at 13.9 years ($p < 0.05$) is detected. The spectrum of MS^- older than 1700 A.D. contains a significant periodicity of 13.9 years whereas the short 4.6-year cycle is lost completely because of postdepositional diffusion of MS^- in the firm zone. Consequently, an aliasing effect of the short-period oscillation on the 13.9-year period is excluded. Note that both frequencies have been found in sea-salt records of the same ice core by Fischer *et al.* [2004] (see below).

[15] It is now possible to assign oscillating atmospheric phenomena to the quasi-periodicities of 4.6 and 13.9 years. Several internal oscillations in ocean/atmosphere dynamics are known, showing variability in the respective period domains. For instance, El Niño–Southern Oscillation (ENSO) variability is known to occur in the period band from 2 to 6 years [An and Wang, 2000; Weiss and Weiss, 1999]. Also the Antarctic Oscillation (AAO) [Thompson and Wallace, 2000], the Antarctic Circumpolar Wave (ACW, 4–5-year periodicities) [White and Peterson, 1996] or the Antarctic Dipole (ADP, 3–5-year periodicity and decadal variability) [Yuan, 2004] are potential forcing patterns. On the basis of the frequency analysis above, none of the above mentioned climate oscillation phenomena can be per se excluded as MS^- forcing parameter. A solar influence, however, seems unlikely. While a ~ 4.6 -year periodicity in sea-salt records has been attributed to sea level pressure (SLP) and, thus, aerosol transport changes related to the ACW by Fischer *et al.* [2004], the origin of the approximately 14-year period remained obscure. Analysis of the circumpolar SLP variability in National Centers for Environmental Prediction–National Center for Atmospheric Research (NCEP/NCAR) reanalysis data, however, indicated despite of the shortness of the records that this is a dominant mode of atmospheric dynamics in this region [Fischer *et al.*, 2004]. Recently, Yuan [2004] found a similar periodicity in indices of surface air temperature (SAT), SLP and sea ice content (SIC) related to the ADP. These indices were constructed in order to capture the ocean and atmospheric variability from the centers of the dipole east and west of the Antarctic Peninsula. Therefore the monthly mean of each parameter in the Atlantic centre (Weddell Sea) was subtracted from that of the Pacific centre (Bellinghousen Sea) of the ADP. Yuan [2004] found significant interannual variability in the ADP indices, similar to the typical ENSO periodicities. Additionally, an approximately 14-year cycle occurred in the SIC, SLP and SAT indices of the ADP. With this result, transport variations by changing pressure patterns connected to the ADP are a likely cause for the observed variations in the MS^- record.

3.2. Forcing by Teleconnection Patterns

[16] Knowing the harmonic components contained in time series does not implicate knowledge about the underlying physical processes leading to the observed changes. Several internal and external forcings with variability in the annual to decadal time span are known and may be responsible for the cycles found in the MS^- record from DML05. There have been a number of publications trying to link MS^- in Antarctic ice core records to

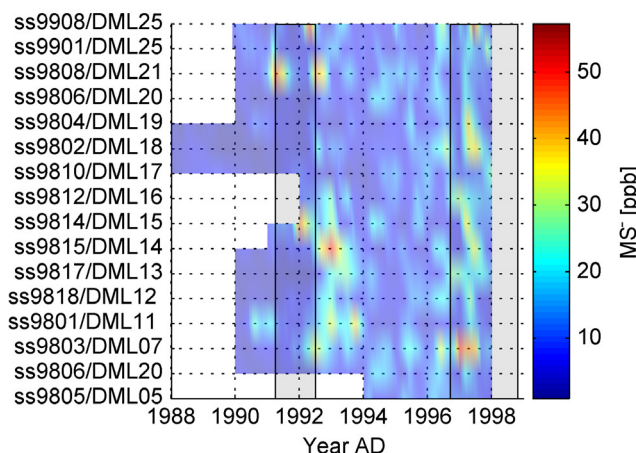


Figure 4. MS^- records of snow pits (labeled by the name and location of the pit, respectively) stacked on a common timescale. The El Niño years 1992 and 1998 and their durations are marked by black lines.

the quasi-periodic El Niño–Southern Oscillation (ENSO) phenomenon [e.g., Legrand, 1997; Legrand and Feniet-Saigne, 1991; Meyerson *et al.*, 2002; Turner, 2004]. The conjecture seems obvious as at many sampling sites MS^- shows increased concentrations in parallel to El Niño years and additionally, meteorological studies show increased moisture transport toward parts of Antarctica during El Niño events [Bromwich *et al.*, 2000]. However, this correlation has not been continuously strong in the past decades [Guo *et al.*, 2004]. Although the causal connection remains obscure, a similar behavior can be seen in the MS^- record of DML snow pits. In most of the time series well pronounced peaks show up in the years 1992 and 1997, coinciding with years of strong and long-lasting (up to 13 month) El Niño events (Figure 4). We rule out that those peaks are artifacts of lower postdepositional loss, as no significant rise of accumulation could be found in the respective years. Also for longer time series in DML shallow cores (not shown) high MS^- concentrations often coincide with El Niño years, however, equally many years of extraordinarily high MS^- concentrations are not coincident with El Niño events.

[17] To unravel potential forcing parameters, the MS^- records from DML were compared to different meteorological parameters for the time span where reliable NCEP/NCAR reanalysis data are available for the SO. As the NCEP/NCAR data prior to 1968 are based on sparse measurements especially in the SO region and show spurious trends [Hines *et al.*, 2000; Marshall and Harangozo, 2000], this early period is not included in this analysis. Although the quantitative information on MS^- deposition is compromised by the postdepositional loss of MS^- , years of extraordinary MS^- concentrations can still be recognized in the time series (see Weller *et al.* [2004] and Figure 4). Thus at least the temporal information of extraordinary MS^- input into the snow pack may contain atmospheric information. Accordingly, a robust method of detecting the imprint of forcing parameters on the MS^- record has to be applied to deduce anomalies for years of extremely high or low MS^- . To identify such years, representative for the

entire study area in DML, the sum of the leading two principal components (PC1 and PC2) from empirical orthogonal function (EOF) analysis of MS^- in the shallow cores from DML03, DML05, DML07 and DML17 was used. EOF analysis, based on principal component analysis, is widely utilized in climate research to determine patterns of shared variability in a set of time series [Meeker *et al.*, 1995; Peixoto and Oort, 1992]. PC1 and PC2 together explain about 80% of the variance of the data set. PC3 and PC4 were not used in order to improve the signal/noise ratio. The extrema were found by searching for local maxima and minima of the sum of PC1 and PC2. Extraordinarily high MS^- concentrations occur in the years 1997, 1994, 1992, 1986, 1981, 1976, 1973 and 1968 whereas extremely low MS^- concentrations were specified in 1993, 1988, 1983, 1978, 1974 and 1970 (Figure 5). Composite anomaly maps in NCEP/NCAR reanalysis data were calculated for years of high minus years of low MS^- concentrations. To avoid the imprint of trends on the composite anomaly maps, the linear trend of the regarded period was removed from the reanalysis data. As possible forcing parameters the anomalies of the NCEP/NCAR reanalysis grid point data sets of meridional wind speed (v_m), SAT and geopotential height at 1000 hPa (gph1000) from 1968 to 1998 were taken into account. Furthermore the variance of SLP data (1–10 days band-pass filtered, representative for the typical lifetime of a cyclonic system at a given point) was used as indicator for storm activity [Fischer *et al.*, 2004].

[18] In Figure 6 (leftmost column) the anomaly maps based on years of high and low MS^- at DML are shown. The v_m pattern reflects the enhanced southward transport from lower latitudes across the Weddell Sea sector to DML. The pattern is consistent with expectations, as the source for MS^- is the SO while air parcels originating from central Antarctica are associated with a lower MS^- content. The transport anomaly is accompanied by a positive SAT anomaly in the eastern Weddell Sea reflecting the simulta-

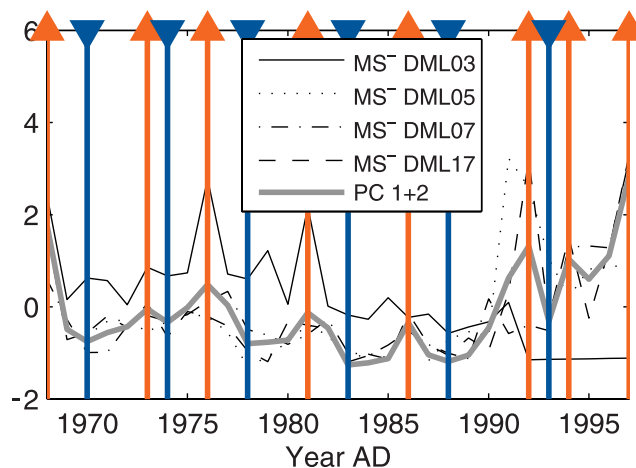


Figure 5. Principal components (PC) 1 + 2 from EOF analysis of MS^- records on the time span 1968–1998. Four shallow ice cores from DML were used in the PC analysis to identify years of high (red) and low (blue) MS^- concentrations. The time series were detrended and normalized to unit variance before calculating the PCs.

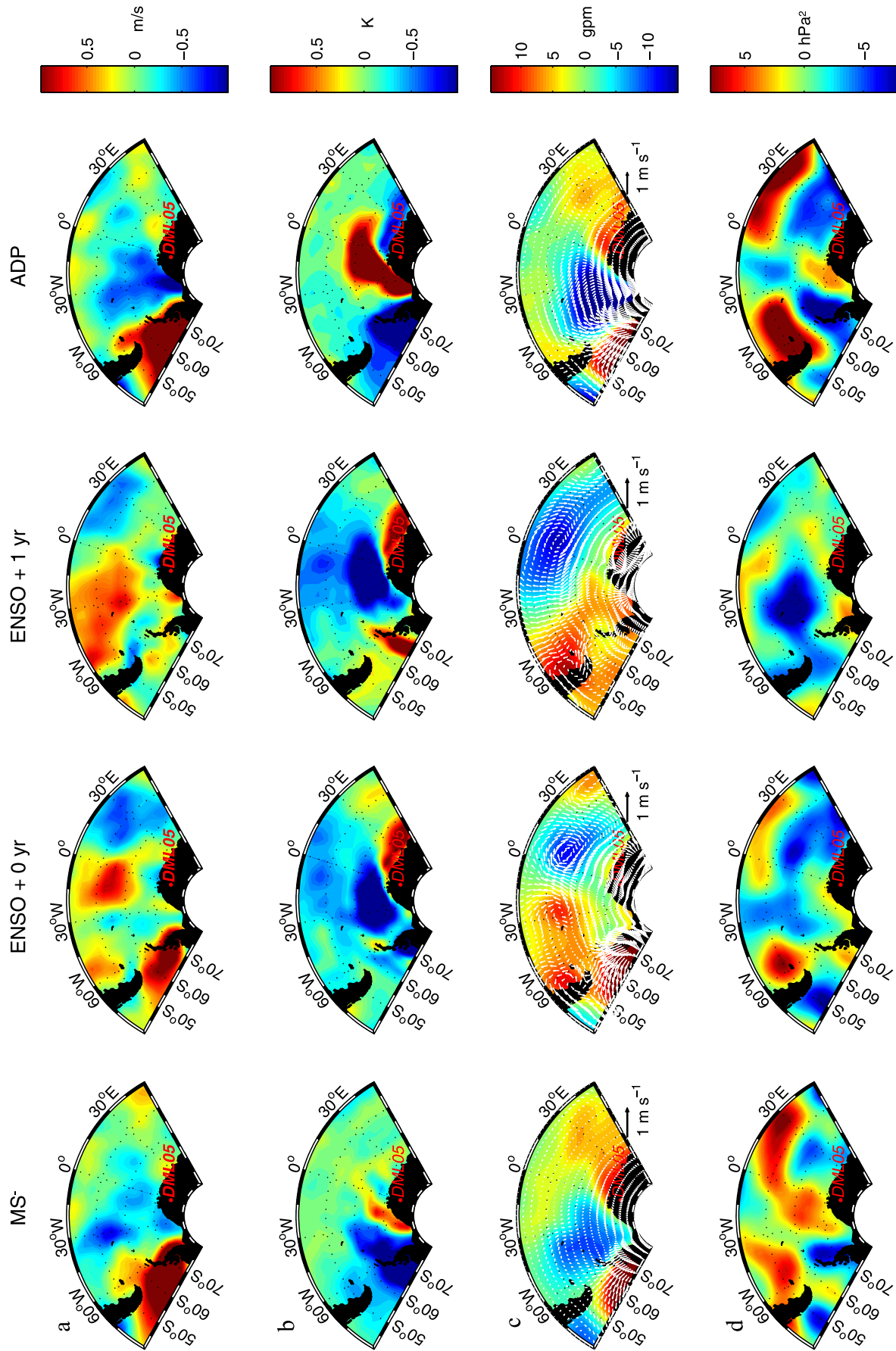


Figure 6

neous positive anomaly in heat flux from the north to Antarctica.

[19] In line with the wind and temperature pattern, the gph1000 anomaly map shows a pronounced low-pressure zone over the Weddell Sea with highest wind speeds where the pressure gradient is largest. In this region also the (summer) storm activity shows positive anomalies. Possibly, intensified cyclonic activity increases the probability for transport of moisture and aerosol to DML. Another conceivable impact of increased gustiness could be an intensified sea-air exchange of DMS, the MS^- precursor. However, when compiling the storm activity composite maps for annual instead of summer anomalies, no increase in storm activity can be found (not shown). This may be due to the summer production maximum of MS^- or, more plausible, be an indicator for transport of MS^- via the free troposphere being more important for DML than transport by cyclones.

[20] Compared to a previous study [Fischer *et al.*, 2004] based on sea-salt components measured at DML, the MS^- based patterns look very similar despite of the different seasonal maximum of sea-salt (higher concentrations in winter/spring) and MS^- (late summer to autumn) concentrations in firn [Göktas *et al.*, 2002]. Accordingly, we can conclude that the influence of these pressure anomalies on aerosol transport to DML is not restricted to a specific season.

[21] To identify or to reject ENSO as forcing for DML MS^- records, the same climate patterns were deduced for years of El Niño (negative Southern Oscillation Index (SOI)) (1997–1998, 1991–1992, 1986–1987, 1982–1983 and 1972–1973) and La Niña (positive SOI) (1988–1990, 1975–1977, 1973–1975 and 1970–1972) in agreement with the periods defined by Trenberth [1997]. Usually El Niño or La Niña events do not start and finish with the beginning and end of a calendar year. Therefore all years of an unusually high and low SOI index are taken into account. The contrast in the ENSO anomaly maps compared to the MS^- anomaly maps is remarkable. Where in the MS^- based maps a southward wind anomaly occurs, the ENSO based map shows anomalous northward wind speeds in the eastern Weddell Sea. Accordingly, a positive temperature anomaly in this region as found in the MS^- based anomaly maps does not exist. The SLP pattern in the Atlantic sector looks almost opposite and the storm activity shows even negative anomalies for El Niño years.

[22] While ENSO is a phenomenon predominantly characteristic for the tropical and subtropical regions, the production and mobilization of MS^- found in DML ice core occurs at middle and high latitudes. Accordingly, it may take some time for the ENSO anomalies to propagate to higher latitudes. This time span might be negligible for atmospheric processes. For oceanic processes, however, the propagation time from low to higher latitudes is signifi-

cantly longer. To ensure, that exceptional high or low MS^- concentrations at DML are not due to lagged ENSO signals, the anomaly maps were also calculated for a shift of 1 year in the ENSO extrema. It is not surprising, that the patterns for the ENSO and the lagged ENSO anomaly maps resemble each other. As most ENSO events encompass more than 1 year, the data on which the maps are based are partly overlapping. Nevertheless, the anomalies revealed in the lagged ENSO anomaly maps are even more pronounced than for ENSO years and even more in conflict with the anomalies based on MS^- . Consequently, a direct influence of ENSO on the DML ice core records of MS^- should be rejected.

[23] Still an option is a teleconnection pattern at the middle and high latitudes that is triggered by ENSO but has its own temporal dynamics. When looking at the gph1000 anomaly map for MS^- a high-pressure anomaly in the Pacific part of the SO occurs simultaneously with the low-pressure anomaly in the Weddell sector. This pressure distribution is typical for the southern midlatitudes and is called the ADP [Yuan and Martinson, 2000]. It is represented by the second empirical orthogonal function (EOF2) of the gph1000 data (Figure 7a), explaining about 10% of the Southern Hemisphere pressure variability and is the second most important pattern in the Southern Hemisphere after the Southern Annular Mode (EOF1). Similar patterns in SAT and sea ice concentrations (SIC) were found and attributed to the ADP, which in part is modulated by ENSO [Yuan, 2004]. Creating dipole indices (DPI) based on the difference of SAT (DPI_{SAT}) and SIC (DPI_{SIC}) anomalies from the centre of the poles of the ADP, Yuan [2004] found dominating periodicities between 3 and 5 years, which he assigned to an atmospheric teleconnection to ENSO. In addition, his analysis showed a large fraction of variance on a decadal scale, in line with the 13.9 years found in the MS^- record in the deeper core section at DML05, which may be induced by long-term ENSO variability (2.8–5.7 and 15–18 years) as found by Mann and Park [1994] in global surface temperatures.

[24] We examined the condition of the atmosphere using anomaly maps for exceptional years of the dipole index (DPI_{GPH}) based on the gph1000 data. The years used were chosen after normalizing the DPI to standard deviation and picking years below (1988, 1974, 1971, 1970) or above (1991, 1986, 1977, 1976, 1968) 1σ (Figure 7b) around the mean of the ADP indices. The similarity to the extrema maps of the stacked MS^- records is extraordinary. In the meridional wind anomalies, the surface air temperature and the surface pressure the patterns of the MS^- maps are accurately reproduced. Also in the summer (JFM) storm activity maps, similar patterns can be found. Indeed not only the spectral behavior and the anomaly maps of MS^- and the ADP are similar, also a comparison of DPI_{SAT} and DPI_{GPH} with MS^- concentrations shows a significant correlation

Figure 6. Leftmost column shows the anomaly maps for years of increased MS^- minus years of decreased MS^- . (a) Annual meridional surface wind anomalies, (b) annual surface air temperature anomalies, (c) annual gph1000 anomalies plus surface wind vector, and (d) SLP JFM storm activity anomalies. Second column shows the anomaly maps for years of El Niño (negative SOI) minus years of La Niña (positive SOI) events. Third column is the same as the second, but for extreme SOI years lagged by 1 year. Rightmost column shows the anomaly map for years where the ADP index DPI_{GPH} is 1σ above minus 1σ below average.

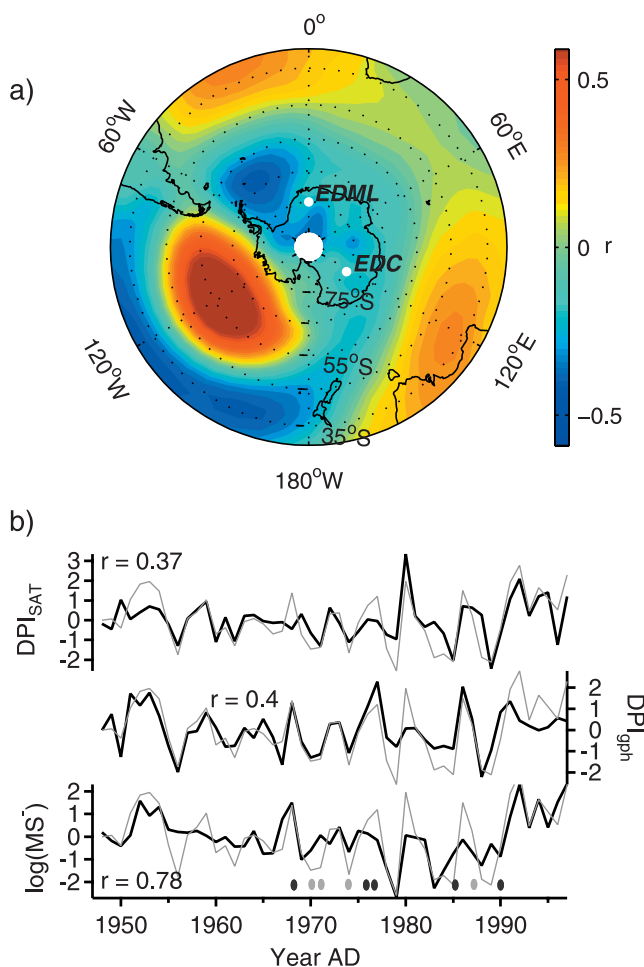


Figure 7. (a) Correlation map of the NCEP/NCAR SLP data with the second principal component from EOF analysis, explaining $\sim 10\%$ of the SLP data variance used; (b) $\log(\text{MS}^-)$ from DML05 together with Antarctic dipole indices for SAT (DPI_{SAT}) and gph1000 (DPI_{GPH}). Both indices are significantly correlated to MS^- on the 99% level. The grey lines show the first principal component of EOF analysis, representing 58% of the total variance. All time series were normalized to unit variance before applying EOF analysis. The years of DPI_{GPH} above or below 1σ are indicated by the black or grey dots.

(Figure 7b). The correlation with the dipole index of geopotential height ($r = 0.4$, $p < 0.05$) can be improved up to $r = 0.5$ by using higher pressure levels in the troposphere that are more representative for aerosol transport toward Antarctica. As the ADP is not the exact counterpart of ENSO in the SO [Yuan, 2004] this outcome is not in contradiction to the previously found different patterns of ENSO and MS^- . This result suggests that MS^- in DML ice cores may be a valid proxy for the interannual ADP variability, as long as postdepositional processes do not disturb the signal. In older DML ice, where the high-frequency information is lost by diffusional smoothing, one might still be able to deduce decadal ADP variability from the MS^- signal.

[25] In terms of their spectral properties the multiannual variability of about 4.6 years could be related to the ADP

or the ACW. However, the decadal variability of around 14 years found in MS^- and sea-salt aerosol [Fischer *et al.*, 2004] deposition in DML cannot be attributed to the ACW. This makes the ADP become the more plausible circulation pattern responsible for transport of aerosol toward DML. As a matter of fact the ADP and the ACW may not be independent. Effectively, the ADP initializes the conditions for SAT and SIC in the Weddell Sea (leading to anomalies in SLP), which then can be propagated by the Circumantarctic Current. This potential connection of the ADP and the ACW may also contribute to our understanding why the ACW has been only partly propagating during the last decades, while during other periods it seems to be a standing wave phenomenon. A further study of the ADP/ACW connection, however, is beyond the scope of this paper.

[26] In summary, the mechanism responsible for a large fraction of variability of MS^- records from DML could be as follows. Triggered by ENSO an anomalous high-pressure system in the Pacific part of the SO forms [Yuan, 2004]. At the same time the low-pressure anomaly in the Weddell Sea sector is reinforced to an enhancement of the ADP pattern. This typical pressure constellation in the Southern Hemisphere west and east of the Drake passage shows a dominant variability from 3 to 5 and around 15 years. The Weddell Sea low-pressure system is responsible for enhanced transport directed to DML. If this weather situation happens during the season of production of DMS by phytoplankton, an increased deposition of MS^- in DML becomes likely.

[27] Regarding the comparatively large fraction of variance in the MS^- data that cannot be assigned to the ADP, various processes such as variability in marine productivity, internal variability in the atmosphere dynamics as well as variability in the deposition and postdeposition processes all contribute to a low signal-to-noise ratio. Furthermore, an interaction of the ADP, causing a large positive SAT anomaly in the Weddell Sea and, thus, a more intense algae bloom is possible as well.

[28] Because of the spatially limited extension of the ADP to the westerly part of the SO (Figure 7b), an influence on cores from other (especially east) Antarctic drilling sites cannot be expected. For example, chemistry records from Dome Summit South, Law Dome, East Antarctica, show no variability in the spectral band of the ADP [Souney *et al.*, 2002]. We therefore conclude that large parts of east Antarctica are unaffected by the ADP. Besides DML, only in West Antarctica an ADP signal should be expected. This is confirmed by Kreutz *et al.* [2000], who found an ADP-like SLP pattern correlated to multivariate ice core chemistry records from Siple Dome in the Amundsen Sea region. Further on, according to Meyerson *et al.* [2002], MS^- from South Pole is correlated to the SIE and to ENSO variability affecting the sea ice coverage. However, as the source region for aerosol transported to South Pole is the Amundsen Sea [Meyerson *et al.*, 2002] west of the main ADP center of action a connection to the ADP may be more straightforward. Further on, we suggest an imprint of the ADP also on southern American regions. As has been shown by tree ring reconstructions of Patagonian precipitation [Villalba *et al.*, 1998], significant variability in the ENSO band (3–6 years) can be found but precipitation is

not clearly connected to ENSO. *Villalba et al.* [1998] also show an ADP-like SLP pattern having an effect on Patagonian precipitation.

[29] In general we suggest future research of atmospheric variability in the western part of the SO to be focused more on ADP than on ENSO variability solely.

3.3. Long-Term Changes in Extreme Values

[30] The composite maps described in section 3.2 were derived from a short period of reliable instrumental data describing the state of the SO atmosphere. A validation of the suggested transport dependency of MS^- on longer timescales would be useful to support our conclusions. Therefore we use the DML05 core covering the past about 1800 years, looking for years of exceptionally high concentrations of MS^- .

[31] An important chemical component able to confirm the transport hypothesis is sea-salt aerosol (here we use Cl^-), measured on the same sample. The source region is approximately the same, but sea-salt aerosol is produced by wind-induced dispersion of seawater. Sea-salt aerosol measured in Antarctic ice cores has been shown to be largely influenced by atmospheric transport processes [*Fischer et al.*, 2004; *Kreutz et al.*, 2000]. Thus, as we consider processes on an annual scale here, a common signal caused by changes in transport efficiency should be visible in MS^- as well as in sea-salt aerosol, although the timing of input is seasonally decoupled.

[32] To identify years of exceptionally high MS^- concentration, an outlier detection routine was applied, described by *Fischer et al.* [1998]. The routine creates a threshold (the median plus 2 times the median of the absolute deviation from the median) using a running window of 100 years, where free parameters were chosen. A total amount of 229 years exceeding the threshold were found (Figure 2). To check, whether years of exceptionally high concentrations of MS^- also show higher concentrations in Cl^- , we performed a t test on logarithmic Cl^- concentrations, comparing the mean concentration of the entire Cl^- record with the mean of the years selected in our outlier analysis. The overall chloride record shows a mean of 51.9 ppb. On the basis of the 99% significance level the t test results in an expected range of the mean from 49.3 to 54.6 ppb for the complete Cl^- record. The mean of the chloride record for years of unusual high MS^- concentrations is 59.8 ppb and thus significantly above the total chloride mean (Figure 2, inlay). Accordingly, this points to somewhat enhanced sea-salt transport for periods of higher MS^- concentrations.

[33] However there is also a large fraction of Cl^- peaks without corresponding peak in MS^- . One possible explanation might be (as, e.g., shown by *Hammer et al.* [1997] for the Byrd core in west Antarctica) peaks in Cl^- that are caused by volcanic eruptions emitting large amounts of HCl into the atmosphere. However, those peaks are supposed to occur sporadically only. Thus only a small part of the large fraction of chloride peaks without correspondent signal in the MS^- record can be attributed to volcano events. More important for the differing number of Cl^- and MS^- peaks seems to be the seasonal decoupling of the MS^- and Cl^- deposition, as, for example, cyclonic events in austral winter, when biological

production of MS^- is low, result only in Cl^- peaks but not in MS^- peaks.

[34] Coinciding variations in MS^- and Cl^- are not found in the extreme values only. Also on longer timescales, similar long-term anomalies can be observed in both records. Such is the period from approximately 1200 to 1600 A.D. (marked in Figure 2 by the shaded box) where an increase in the frequency of Cl^- peaks appears and at the same time also the average MS^- concentration is increased. Accordingly, we can speculate that this interval was characterized by an enhanced deep pressure center in the Weddell Sea due to an intensified ADP pattern.

[35] Additional hints of changing transport efficiency in the Pacific sector of the SO come from the Siple Dome chemistry record covering the past 1150 years [*Kreutz et al.*, 2000]. Around 1400 A.D. an increase in aerosol deposited at the drilling site was attributed to atmospheric transport processes, especially due to an intensification of the Amundsen Sea low-pressure system. Contemporaneously, an increase of decadal variability was found in the chemistry record at this period and connected to increased ENSO activity during the Little Ice age from about 1400 to 1900 A.D. [*Anderson*, 1992]. On the basis of our analysis, we suggest a link of the periods of increased sea-salt input to DML as well as to Siple Dome via the ADP.

4. Conclusion

[36] This work contributes to the understanding of processes underlying the variations in MS^- of ice cores from DML. In spite of postdepositional processes occurring at low-accumulation sites, there is still some information left in the records. In the recent 300 years, interannual variability is still present. The older part of the core only contains variability above wavelengths of 10 years. Spectral analysis of the younger part of the MS^- record shows significant variability around 4.6 years. A period of about 14 years is dominating the older part of the record but is also visible in the upper section. These periods coincide with previously found variability in sea-salt records from DML05 [*Fischer et al.*, 2004] supporting common atmospheric circulation patterns dominating the transport of sea-salt and marine biogenic aerosol from their common source areas to the inland plateau of DML.

[37] Atmospheric anomaly maps based on the NCEP/NCAR reanalysis data exhibit consistent patterns, linking high MS^- concentrations with enhanced poleward transport of air masses, which might be additionally connected to enhanced bioproduction in the Weddell Sea sector. A comparison of climate patterns for years of high and low MS^- with years of El Niño and La Niña shows no similarity; consequently, a direct coupling of ENSO and MS^- records from DML is dismissed. However, studies of ENSO teleconnection processes claim the ADP as being triggered by El Niño/La Niña conditions in the tropical Pacific [*Yuan*, 2004]. The pronounced differences in atmospheric states of the Atlantic and the Pacific sector related to the ADP are consistent with composite patterns found for extreme MS^- years. We suggest that the ADP promotes transport of MS^- and sea salt onto DML by influencing transport pathways. Thus the attribution of sea-salt aerosol

transport to the ACW by Fischer *et al.* [2004] has to be refined. In fact SLP anomalies in the Weddell Sea for years of extraordinary sea-salt concentrations in DML ice cores are in line with the ACW pattern, but the underlying trigger of the anomalies appears to be driven by the ADP. A possible initialization of the ACW by changes in SLP across the Antarctic Peninsula should be addressed in more detail in future climatological studies.

[38] Investigation of years of extremely high MS^- concentration in our intermediate ice core record points to more efficient transport processes, as in years of peaking MS^- on average also significantly higher concentrations of chloride can be found. The evaluation of extreme events in the long record is based on more events and thus delivers more robust results. In addition, a period of frequently occurring peaks in Cl^- from approximately 1200 to 1600 A.D. concurs with a period of increased MS^- background concentration, additionally supporting an effect of enhanced transport on DML MS^- and sea-salt records.

[39] **Acknowledgments.** This work is contribution 128 to the “European Project for Ice Coring in Antarctica” (EPICA), a joint European Science Foundation (ESF)/EU scientific programme, funded by the European Commission (EPICA-MIS) and by national contributions from Belgium, Denmark, France, Germany, Italy, Netherlands, Norway, Sweden, Switzerland, and the United Kingdom. NCEP reanalysis data were provided by the NOAA-CIRES Climate Diagnostics Center, Boulder, Colorado, USA, from their Web site at <http://www.cdc.noaa.gov/>. We would like to thank the unknown reviewers, who helped to improve the scope of this study significantly.

References

- An, S. I., and B. Wang (2000), Interdecadal change of the structure of the ENSO mode and its impact on the ENSO frequency, *J. Clim.*, *13*, 2044–2055, doi:10.1175/1520-0442(2000)013<2044:ICOTSO>2.0.CO;2.
- Anderson, R. Y. (1992), Long term changes in the frequency of occurrence of El Niño events, in *El Niño: Historical and Paleoclimatic Aspects of the Southern Oscillation*, edited by H. D. Diaz and V. Markgraf, pp. 193–200, Cambridge Univ. Press, New York.
- Andreae, M. O., and P. J. Crutzen (1997), Atmospheric aerosols: Biogeochemical sources and role in atmospheric chemistry, *Science*, *276*, 1052–1058, doi:10.1126/science.276.5315.1052.
- Ayers, G. P., and R. W. Gillett (2000), DMS and its oxidation products in the remote marine atmosphere: Implications for climate and atmospheric chemistry, *J. Sea Res.*, *43*, 275–286, doi:10.1016/S1385-1101(00)00022-8.
- Barnes, P. R. F., E. W. Wolff, H. M. Mader, R. Udisti, E. Castellano, and R. Röthlisberger (2003), Evolution of chemical peak shapes in the Dome C, Antarctica, ice core, *J. Geophys. Res.*, *108*(D3), 4126, doi:10.1029/2002JD002538.
- Bates, T., J. Calhoun, and P. Quinn (1992), Variations in the methanesulfonate to sulfate molar ratio in submicrometer marine aerosol particles over the southern Pacific Ocean, *J. Geophys. Res.*, *97*, 9859–9865.
- Bromwich, D. H., A. N. Rogers, P. Kallberg, R. I. Cullather, J. W. C. White, and K. J. Kreutz (2000), ECMWF analyses and reanalyses depiction of ENSO signal in Antarctic precipitation, *J. Clim.*, *13*, 1406–1420, doi:10.1175/1520-0442(2000)013<1406:EAARDO>2.0.CO;2.
- Brown, A. (1976), Microbial water stress, *Bacteriol. Rev.*, *40*, 803–846.
- Cosme, E., F. Hourdin, C. Genthon, and P. Martinerie (2005), Origin of dimethylsulfide, non-sea-salt sulfate, and methanesulfonic acid in eastern Antarctica, *J. Geophys. Res.*, *110*, D03302, doi:10.1029/2004JD004881.
- Curran, M. A. J., A. S. Palmer, T. D. Van Ommen, V. I. Morgan, K. Phillips, A. J. McMorrow, and P. A. Mayewski (2002), Post-depositional movement of methanesulphonic acid at Law Dome, Antarctica, and the influence of accumulation rate, *Ann. Glaciol.*, *35*, 333–339.
- Curran, M. A. J., T. D. van Ommen, V. I. Morgan, K. L. Phillips, and A. S. Palmer (2003), Ice core evidence for Antarctic sea ice decline since the 1950s, *Science*, *302*, 1203–1206, doi:10.1126/science.1087888.
- de Angelis, M., and M. Legrand (1995), Preliminary investigations of post depositional effects on HCl, HNO₃, and organic acids in polar firn layers, in *Ice Core Studies of Global Biogeochemical Cycles*, NATO ASI Ser., Ser. I, vol. 30, edited by R. J. Delmas, pp. 361–381, Springer, New York.
- Delmas, R. J., P. Wagon, K. Goto-Azuma, K. Kamiyama, and O. Watanabe (2003), Evidence for the loss of snow-deposited MSA to the interstitial gaseous phase in central Antarctic firn, *Tellus, Ser. B*, *55*, 71–79, doi:10.1034/j.1600-0889.2003.00032.x.
- Fischer, H., D. Wagenbach, and J. Kipfstuhl (1998), Sulfate and nitrate firn concentrations on the Greenland Ice Sheet: 2. Temporal anthropogenic deposition changes, *J. Geophys. Res.*, *103*, 21,935–21,942, doi:10.1029/98JD01886.
- Fischer, H., F. Traufetter, H. Oerter, R. Weller, and H. Miller (2004), Prevalence of the Antarctic Circumpolar Wave over the last two millennia recorded in Dronning Maud Land ice, *Geophys. Res. Lett.*, *31*, L08202, doi:10.1029/2003GL019186.
- Ghil, M., et al. (2002), Advanced spectral methods for climatic time series, *Rev. Geophys.*, *40*(1), 1003, doi:10.1029/2000RG000092.
- Göktas, F., H. Fischer, H. Oerter, R. Weller, S. Sommer, and H. Miller (2002), A glacio-chemical characterization of the new EPICA deep-drilling site on Amundsenisen, Dronning Maud Land, Antarctica, *Ann. Glaciol.*, *35*, 347–354.
- Gondwe, M., M. Krol, W. Gieskes, W. Klaassen, and H. de Baar (2003), The contribution of ocean-leaving DMS to the global atmospheric burdens of DMS, MSA, SO₂, and NSS SO₄⁻, *Global Biogeochem. Cycles*, *17*(2), 1056, doi:10.1029/2002GB001937.
- Guo, Z. C., D. H. Bromwich, and K. M. Hines (2004), Modeled Antarctic precipitation. Part II: ENSO modulation over West Antarctica, *J. Clim.*, *17*, 448–465, doi:10.1175/1520-0442(2004)017<0448:MAPPIE>2.0.CO;2.
- Hammer, C. U., H. B. Clausen, and C. C. Langway (1997), 50,000 years of recorded global volcanism, *Clim. Change*, *35*, 1–15, doi:10.1023/A:1005344225434.
- Hines, K. M., D. H. Bromwich, and G. J. Marshall (2000), Artificial surface pressure trends in the NCEP-NCAR reanalysis over the Southern Ocean and Antarctica, *J. Clim.*, *13*, 3940–3952, doi:10.1175/1520-0442(2000)013<3940:ASPTIT>2.0.CO;2.
- Isaksson, E., W. Karlen, P. Mayewski, M. Twickler, and S. Whitlow (2001), A high-altitude snow chemistry record from Amundsenisen, Dronning Maud Land, Antarctica, *J. Glaciol.*, *47*, 489–496.
- Karsten, U., K. Kück, C. Vogt, and G. O. Kirst (1996), Dimethylsulfonio-propionate production in phototrophic organisms and its physiological function as a cryoprotectant, in *Biological and Environmental Chemistry of DMSP and Related Sulfonium Compounds*, edited by R. P. Kiene et al., pp. 143–153, Springer, New York.
- Kohfeld, K. E., C. Le Quere, S. P. Harrison, and R. F. Anderson (2005), Role of marine biology in glacial-interglacial CO₂ cycles, *Science*, *308*, 74–78, doi:10.1126/science.1105375.
- Kreutz, K. J., P. A. Mayewski, I. I. Pittalwala, L. D. Meeker, M. S. Twickler, and S. I. Whitlow (2000), Sea level pressure variability in the Amundsen Sea region inferred from a West Antarctic glaciochemical record, *J. Geophys. Res.*, *105*, 4047–4059, doi:10.1029/1999JD901069.
- Legrand, M. (1997), Ice-core records of atmospheric sulphur, *Philos. Trans. R. Soc. London, Ser. B*, *352*, 241–250, doi:10.1098/rstb.1997.0019.
- Legrand, M., and C. Feniet-Saigne (1991), Methanesulfonic acid in south polar snow layers: A record of strong El Niño?, *Geophys. Res. Lett.*, *18*, 187–190, doi:10.1029/90GL02784.
- Legrand, M., A. Leopold, and F. Dominec (Eds.) (1996), Acidic gases (HCl, HF, HNO₃, HCOOH, and CH₃COOH): A review of ice core data and some preliminary discussions on their air-snow relationships, in *Processes of Chemical Exchange Between the Atmosphere and Polar Snow*, NATO ASI Ser., Ser. I, vol. 43, edited by E. W. Wolff and R. C. Bales, pp. 19–43, Springer, New York.
- Mann, M. E., and J. Park (1994), Global-scale modes of surface temperature variability on interannual to century timescales, *J. Geophys. Res.*, *99*, 25,819–25,834, doi:10.1029/94JD02396.
- Marshall, G. J., and S. A. Harangozo (2000), An appraisal of NCEP/NCAR reanalysis MSLP data viability for climate studies in the South Pacific, *Geophys. Res. Lett.*, *27*, 3057–3060, doi:10.1029/2000GL011363.
- Meeker, L. D., P. A. Mayewski, and P. Bloomfield (1995), A new approach to glaciochemical time series analysis, in *Ice Core Studies of Global Biogeochemical Cycles*, NATO ASI Ser., Ser. I, vol. 30, edited by R. J. Delmas, pp. 383–400, Springer, New York.
- Meyerson, E. A., P. A. Mayewski, K. J. Kreutz, L. D. Meeker, S. I. Whitlow, and M. S. Twickler (2002), The polar expression of ENSO and sea-ice variability as recorded in a South Pole ice core, *Ann. Glaciol.*, *35*, 430–436.
- Minikin, A., D. Wagenbach, W. Graf, and J. Kipfstuhl (1994), Spatial and seasonal variations of the snow chemistry at the central Filchner-Ronne ice shelf, Antarctica, *Ann. Glaciol.*, *20*, 283–290.
- Minikin, A., M. Legrand, J. Hall, D. Wagenbach, C. Kleefeld, E. W. Wolff, E. Pasteur, and F. Ducroz (1998), Sulfur-containing species (sulfate and methanesulfonate) in coastal Antarctic aerosol and precipitation, *J. Geophys. Res.*, *103*, 10,975–10,990, doi:10.1029/98JD00249.

- Oerter, H., W. Graf, F. Wilhelms, A. Minikin, and H. Miller (1999), Accumulation studies on Amundsenisen, Dronning Maud Land, Antarctica, by means of tritium, dielectric profiling and stable-isotope measurements: First results from the 1995–96 and 1996–97 field seasons, *Ann. Glaciol.*, **29**, 1–9.
- Oerter, H., F. Wilhelms, F. Jung-Rothenhäusler, F. Göktaş, H. Miller, W. Graf, and S. Sommer (2000), Accumulation rates in Dronning Maud Land, Antarctica, as revealed by dielectric-profiling measurements of shallow firn cores, *Ann. Glaciol.*, **30**, 27–34.
- Peixoto, J. P., and H. Oort (1992), *Physics of Climate*, 520 pp., Am. Inst. of Phys., New York.
- Reijmer, H., R. van den Broeke, and M. P. Scheele (2002), Air parcel trajectories and snowfall related to five deep drilling locations in Antarctica based on the ERA-15 dataset, *J. Clim.*, **15**, 1957–1968, doi:10.1175/1520-0442(2002)015<1957:APTASR>2.0.CO;2.
- Röthlisberger, R., et al. (2002), Nitrate in Greenland and Antarctic ice cores: A detailed description of post-depositional processes, *Ann. Glaciol.*, **35**, 209–216.
- Röthlisberger, R., R. Mulvaney, E. W. Wolff, M. A. Hutterli, M. Bigler, M. de Angelis, M. E. Hansson, J. P. Steffensen, and R. Udisti (2003), Limited dechlorination of sea-salt aerosols during the last glacial period: Evidence from the European Project for Ice Coring in Antarctica (EPICA) Dome C ice core, *J. Geophys. Res.*, **108**(D16), 4526, doi:10.1029/2003JD003604.
- Sieburth, J. (1960), Acrylic acid, an ‘antibiotic’ principle in phaeocystis blooms in Antarctic waters, *Science*, **132**, 676–677.
- Sommer, S., C. Appenzeller, R. Röthlisberger, M. A. Hutterli, B. Stauffer, D. Wagenbach, H. Oerter, F. Wilhelms, H. Miller, and R. Mulvaney (2000), Glacio-chemical study spanning the past 2 kyr on three ice cores from Dronning Maud Land, Antarctica: 1. Annually resolved accumulation rates, *J. Geophys. Res.*, **105**, 29,411–29,421, doi:10.1029/2000JD004449.
- Souney, J. M., P. A. Mayewski, I. D. Goodwin, L. D. Meeker, V. Morgan, M. A. J. Curran, T. D. van Ommen, and A. S. Palmer (2002), A 700-year record of atmospheric circulation developed from the Law Dome ice core, East Antarctica, *J. Geophys. Res.*, **107**(D22), 4608, doi:10.1029/2002JD002104.
- Sunda, W., D. J. Kieber, R. P. Kiene, and S. Huntsman (2002), An antioxidant function for DMSP and DMS in marine algae, *Nature*, **418**, 317–320, doi:10.1038/nature00851.
- Thomson, D. J. (1982), Spectrum estimation and harmonic analysis, *Proc. IEEE*, **70**, 1055–1096.
- Thompson, D. W. J., and J. M. Wallace (2000), Annular modes in the extratropical circulation. Part I: Month-to-month variability, *J. Clim.*, **13**, 1000–1016, doi:10.1175/1520-0442(2000)013<1000:AMITEC>2.0.CO;2.
- Traufetter, F., H. Oerter, H. Fischer, R. Weller, and H. Miller (2004), Spatio-temporal variability in volcanic sulphate deposition over the past 2 kyr in snow pits and firn cores from Amundsenisen, Antarctica, *J. Glaciol.*, **50**, 137–146.
- Trenberth, K. E. (1997), The definition of El Niño, *Bull. Am. Meteorol. Soc.*, **78**, 2771–2777, doi:10.1175/1520-0477(1997)078<2771:TDOENO>2.0.CO;2.
- Turner, J. (2004), The El Niño—Southern Oscillation and Antarctica, *Int. J. Climatol.*, **24**, 1–31, doi:10.1002/joc.965.
- Villalba, R., E. R. Cook, G. C. Jacoby, R. D. D’Arrigo, R. Villalba, T. T. Veblen, and P. D. Jones (1998), Tree-ring based reconstructions of northern Patagonia precipitation since AD 1600, *Holocene*, **8**, 659–674.
- von Glasow, R., and P. J. Crutzen (2004), Model study of multiphase DMS oxidation with a focus on halogens, *Atmos. Chem. Phys.*, **4**, 589–608.
- Wagon, P., R. J. Delmas, and M. Legrand (1999), Loss of volatile acid species from upper firn layers at Vostok, Antarctica, *J. Geophys. Res.*, **104**, 3423–3431, doi:10.1029/98JD02855.
- Weiss, J. P., and J. B. Weiss (1999), Quantifying persistence in ENSO, *J. Atmos. Sci.*, **56**, 2737–2760, doi:10.1175/1520-0469(1999)056<2737:QPIE>2.0.CO;2.
- Weller, R., F. Traufetter, H. Fischer, H. Oerter, C. Piel, and H. Miller (2004), Postdepositional losses of methane sulfonate, nitrate, and chloride at the European Project for Ice Coring in Antarctica deep-drilling site in Dronning Maud Land, Antarctica, *J. Geophys. Res.*, **109**, D07301, doi:10.1029/2003JD004189.
- White, W. B., and R. G. Peterson (1996), An Antarctic circumpolar wave in surface pressure, wind, temperature and sea-ice extent, *Nature*, **380**, 699–702, doi:10.1038/380699a0.
- Wolfe, G., M. Steinke, and G. Kirst (1997), Grazing-activated chemical defense in a unicellular marine alga, *Nature*, **387**, 894–897, doi:10.1038/43168.
- Yuan, X. J. (2004), ENSO-related impacts on Antarctic sea ice: A synthesis of phenomenon and mechanisms, *Antarct. Sci.*, **16**, 415–425, doi:10.1017/S0954102004002238.
- Yuan, X. J., and D. G. Martinson (2000), Antarctic sea ice extent variability and its global connectivity, *J. Clim.*, **13**, 1697–1717, doi:10.1175/1520-0442(2000)013<1697:ASIEVA>2.0.CO;2.

H. Fischer, F. Fundel, H. Miller, H. Oerter, and R. Weller, Alfred Wegener Institute for Polar and Marine Research, Columbusstrasse, D-27568 Bremerhaven, Germany. (ffundel@awi-bremerhaven.de)
F. Traufetter, Prinsengracht 596/II, NL-1017 KS Amsterdam, Netherlands.